Aalborg University

Master Thesis Project

Modified Wood for Low-Grade Heat Harvesting

Written by:

Mor Diop

Supervised by:

Aamer Ali

Cejna Anna Quist-Jensen

Department of Chemistry and Bioscience

9th-10th semester

June 3rd, 2024

Modified Wood for low-grade heat harvesting

Mor Diop

Master Thesis Project 2024

Chemistry and Bioscience
Aalborg University
http://www.aau.dk

AALBORG UNIVERSITY
STUDENT REPORT

Title:
Modified wood for low-grade heat harvesting.

Project Period:
Autumn semester 2023- Spring semester 2024

Participants:

Mor Diop

Supervisors:
Aamer Ali(AAU)
Cejna Anna Quist-Jensen(AAU)

Page Numbers: 42

Date of Completion:
June 3, 2024

Abstract:

Around 40% of the world's population faces severe freshwater shortages, projected to reach three-fourths by 2050. This scarcity poses challenges for potable, irrigation, and industrial water needs, in different parts of the world including Southern Europe.The increasing demand for sustainable energy solutions has led to significant interest in the development of materials capable of efficiently harvesting low-grade heat from the environment. To cope with the challenge, freshwater extraction from seawater or brackish water has gained significant traction. Current desalination systems; however, depend on high-grade energy sources such as fuel or electricity, making them expensive and resulting in a significant CO_2 footprint. Countries like Saudi Arabia devote up to 20% of their oil output to desalination, expected to double by 2050. Therefore, the development of energy-efficient and eco-friendly desalination and wastewater treatment methods is crucial.

Preface

This report is written as 9-10th semester,master thesis project ,at the Department of Chemistry and Bioscience at Aalborg University supervised by Cejna Anna Quist-Jensen and Aamer Ali. The report's title is "*Modified wood for low grade heat harvesting*" and covers 60 ETCS points.

Experiments are performed at Aalborg University at the Department of Chemistry and Bioscience at Fredrik Bajers Vej 7H in the laboratories north and south on levels 3. The abbreviation are found on page iii, and the symbols are found on page iv. The figures and eventual tables presented in this project, are created by the author unless else is stated.For reference and bibliography Harvard citation method is used.

Abbreviations

Abbreviation	Definition
DW	Delignified Wood
EDL	Electrical Double Layer
IH	Inner Helmholtz
OH	Outer Helmholtz
S	Slipping Plane
FSP	Fiber Saturation Point
SEM	Scanning electron microscope
FT-IR	Fourier-transform infrared spectroscopy
S1	Outer Layer
S2	Middle Layer
S3	Inner Layer
EtOH	Ethanol
H_2O_2	Hydrogen Peroxide
$NaClO_2$	Sodium chlorite
NaCl	Sodium Chloride
V_o	Voltage Output

Symbols

Symbols	Definition
W	Watt
ζ	Zeta Potential
ψ_0	Diffuse Layer Potential
ΔP	Differential Pressure
ΔV	Differential Potential
ε	Dielectric coefficient
ε_0	Permittivity
η	Viscosity
σ	Fluid conductivity
κ	Debye Huckel parameter
N_a	Avogadro number
I	Ionic Strength
k_b	Boltzmann constant
T	Temperature
λ_D	Debye Length
e	Elementary Charge
z_i	Ion valence
c_i	Ion concentration
x	Surface Distance
S_c	Seebeck Coefficient

Contents

1 Introduction

Against the backdrop concerning ,the severe depletion of traditional fossil fuels and the requirements for sustainable development, harvesting energy from the ambient environment is attracting intensive attention from researchers .Various generators, such as thermoelectric, piezoelectric/triboelectric and electrokinetic generators have been designed to convert renewable thermal and mechanical energy in the ambiance to electricity.

The electricity generating processes of those generators and some electrokinetic generators, are not spontaneous and require the consumption of additional mechanical energy to maintain the continuity of the power generation. Therefore, spontaneous methods of electricity harvesting that only utilize ambient energy, have been widely explored in recent year[1].

Nowadays, the most developed sustainable energy source is hydropower, which produces about 17% of global electricity [2]. Water is not only vital to life but also represents the largest carrier of energy on the Earth.
Covering 71% of the Earth's surface, water consumes about 35% of the solar energy received by the Earth, corresponding to a remarkable 60 petawatts (10^{15} W).
If just a small portion of the tremendous energy contained in water could be harvested, it would readily satisfy the global energy demand of 18 terawatts (10^{12}W) .
Yet, unlike other energy sources (for example wind or solar energy), water energy evolves into a rich variety of forms that dominate the energy transfer occurring in various natural phenomena.[3]

In the last two decades, an alternative form of utilizing hydropower has emerged, which is based on electrokinetic phenomena induced by osmotic pressure.[2]

The conversion of ambient thermal energy into electricity from the nanomaterials based nanogenerator has been demonstrated to be significant potential for several applications, especially which can be driven by the ubiquitous, spontaneous process of water evaporation[4]. Water transport and evaporation in porous materials has been

extensively studied and applied for example in food and earth sciences, and the theory has since been applied to solar steam generation with porous materials. However, the connection between the water evaporation and electricity generation in a porous film remains poorly understood.
Water evaporation is a spontaneous phenomenon occurring continuously in the natural environment. It has recently been proved that water evaporation can generate electric energy based on the electrokinetic effect.
When water molecules flow through narrow capillary channels with a charged surface driven by the capillary force and water evaporation, the counter ions with opposite charges in the electric double layer (EDL) can move together with the water molecules, resulting in the formation of electric potential and current.On the basis of the above mechanism, various nanoporous materials for water evaporation-induced electricity have appeared successively[5].

Although the microscopic mechanism of the water flow and subsequent generation of streaming current inside the capillary channels of porous materials has been studied both via first principles and in experimental settings, little work has been conducted to understand the underlying physics of the porous material on the scale of complete devices, even if such information is crucial for the design and optimization of large-scale implementations of evaporation powered nanogenerators[6].

2 | Problem Statement

It is within this context that the current project seeks to address and transcend these challenges.

The research aims to investigate and develop methods to effectively convert low-grade environmental heat, such as ambient heat, into usable forms of power and water production. This could involve utilizing modified wood materials and structures to harvest and convert this low-grade heat through thermoelectric, piezoelectric, triboelectric, or electrokinetic effects for wood based power system.

In this circumstance, we employed natural wood to harvest electricity from water evaporation based on the streaming potential/current mechanism. Natural wood has an intrinsic anisotropic three dimensional continuous microchannel structure; thus, the hydrodynamic resistance is relatively low, which may lead to a high streaming current. By using this resource-abundant material, wood, the fabrication cost is low and the process is easy to be scalable[2].
The goal would be to create sustainable and efficient systems that can generate electricity and produce water from readily available environmental heat sources.
This would help reduce reliance on fossil fuels and provide alternative means of power and water generation.
.

3 | Theory

3.1 Wood as mimic of membranes

Wood is a renewable, biodegradable, environmental friendly, and natural material[7], and can be seen as a complex 3D composite of bio polymers composed of an interconnected network of cellulose, hemicelluloses, and lignin, as well as various amounts of extractives and inorganics within different wood species[8]. Wood is an attractive material for research due to its unique anisotropic and hygroscopic properties. The anisotropic nature of wood, where its mechanical properties vary depending on the direction of the grain(showed in Fig.3.1 , makes it an interesting subject for studying the relationship between microstructure and macroscopic behavior.

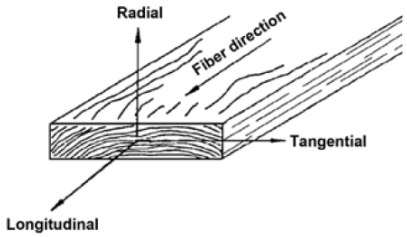

Figure 3.1: Schematic illustration of three principal axes of wood with respect to grain direction,depicted from [9]

Additionally, wood's hygroscopic properties, which allow it to absorb and release moisture, make it a valuable material for understanding the effects of environmental conditions on material properties these properties, combined with wood's natural aesthetic appeal make it an attractive and widely studied material in various fields, including engineering and material science.

Wood nanotechnologies are not only associated with extraction and use of nanocellulose or lignin but also with tailoring and functionalizing the hierarchical nanostructure of bulk wood for functional materials. Applying these technologies allow wood

or cellulose-based porous materials to be used as templates with favorable mechanical and electrical performances[7]

The Woodcell is structured in two walls and the middle lamella:
The middle lamella is a layer that has the function to cement the primary wall cells. The primary wall is very thin and generally has a thickness of around 100nm. The secondary cell wall is typically very thick,rigid,and inelastic. Structurally,the secondary cell wall can be further divided into three layers:
S1(outer) , S2 (middle), and S3 (inner) lamella, as showed in the Fig.3.2.
The three parts are classified due to the different arrangements of cellulose microfibrils. The S1 layer is the thinnest of the layers, representing just 5% to 10% of the total thickness of the cell wall. The S2 layer is the thickest layer,accounting for 75% to 85% of the total thickness of the cell wall and therefore is the most important with regard to mechanical support[10].

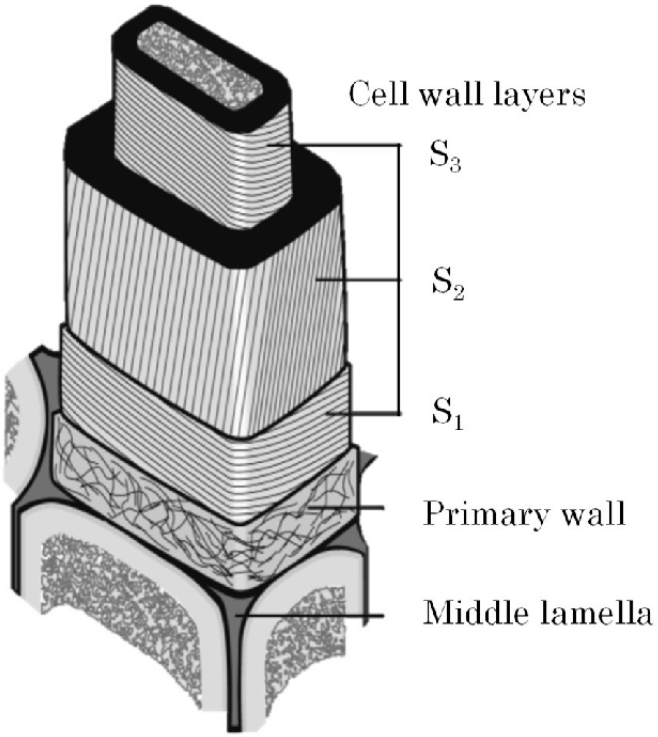

Figure 3.2: Schematic illustration of the wood structure : Middle Lamella, Primary and Secondary Cell Wall (and wall sub division); structure depicted from [11]

The primary wall is a very thin and elastic layer,which is capable of growth and expansion.It can be generally taken that the primary cell wall functions as a scaffold to

support the whole cell forms.The primary cell walls contain cellulose,hemicellulose, pectins,and structural proteins on the basis of their dry mass.

In primary and secondary walls, cellulose acts as a framing material. Cellulose microfibrils are arranged within a hemicellulose matrix, marginally covered by lignin, which acts as incrusting material. The intercellular regions between cell walls (middle lamella) are composed of 70–80% lignin by weight and act as a cementing material to provide cell wall rigidity against growth stresses and other external loads[8].

Although the composition of secondary cell walls varies widely among different species and cell types,the secondary cell walls usually contain cellulose, hemicelluloses, and lignin as showed in Fig. 3.3.

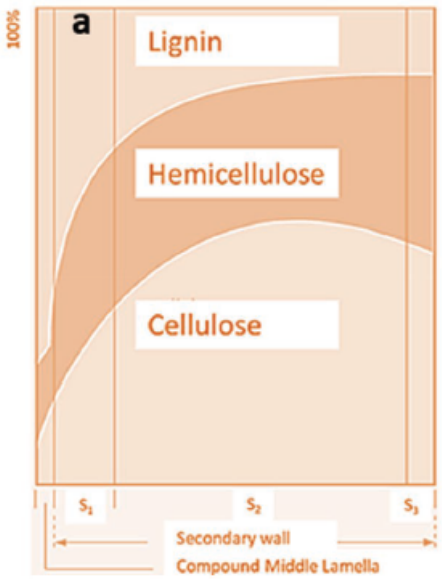

Figure 3.3: Schematic illustration of cellulose,hemicellulose and lignin distribution in the Secondary Wall and Middle Lamella, depicted from [12]

Cellulose makes up to 40% dry mass of secondary cell walls and is present as microfibrils. In addition to cellulose,hemicelluloses are important components in the secondary cell wall for the structure formation and stabilization.

Lignin is another major constituent within secondary cell walls,and accounts for about 10–25% of total plant dry matter[10].
The chemical components of wood are mainly cellulose, hemicelluloses, and lignin, which comprise ~40%, 15–35%, and 20–30% of the mass of wood, respectively[8].

3.1.1 Cellulose

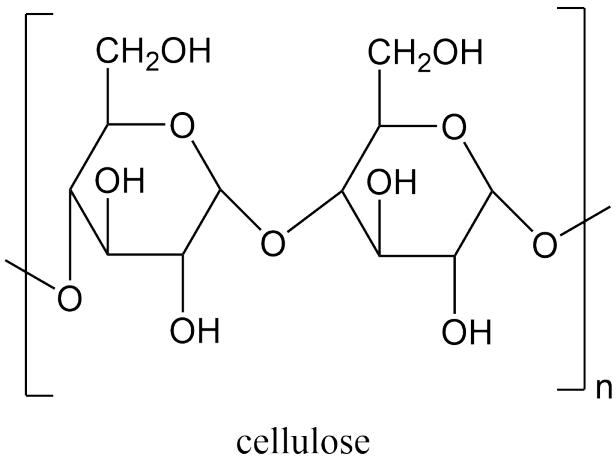

Figure 3.4: Schematic illustration of the cellulose structure,drawn with ChewDraw.

As one of the most abundant bio polymers in the world,the production of cellulose by photosynthesis is estimated to be 10^{11} – 10^{12} tons per year. As one of the typical polysaccharides ,cellulose has a linear polymeric backbone consisting of anhydroglucose units. The units are connected between their C1 and C4 carbons of two adjacent anhydroglucose units by forming β-(1,4)-glycosidic linkages. It is an essential structural cell component for many organisms in addition to plants,such as bacteria,algae and animals. Within plant secondary cell walls,cellulose chains tend to organize into ribbon-like,para crystalline structures by further forming cellulose micro and macrofibrils that are embedded in a matrix of diverse polysaccharides and glycoproteins[10].

3.1.2 Hemicelluloses

The second most abundant polymer after cellulose is hemicellulose which , shows a lack of crystalline structure mainly due to the highly branched structure, and the presence of acetyl groups connected to the polymer chain[12] as showed in the Fig.3.5:

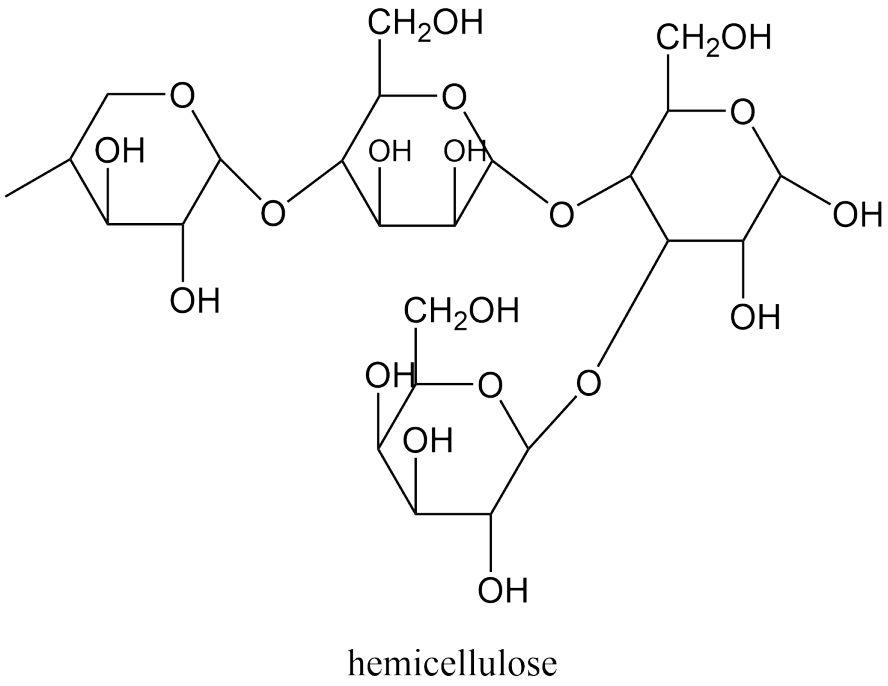

Figure 3.5: Schematic illustration of the hemicellulose structure,drawn with ChewDraw.

and due this is amorphous nature, degrade quickly. In contrast to cellulose containing only D-anhydroglucose units, the complex hemicelluloses structures include various anhydro sugar units with diverse proportions and substituents[10]. The backbone of the hemicellulose polymer is built up by sugar monomers like xylans, mannans and glucans; with xylans being the principal constituents of the hemicelluloses in hardwood, and mannans being the dominant hemicelluloses in softwoods. Cellulose and hemicellulose binds tightly with non covalent attractions to the surface of each cellulose microfibril. Among other important aspects, the capacity to permeate water, and thus, provide flexibility and support in the cell wall[8].

3.1.3 Lignin

Lignin is generally the most complex and smallest fraction, representing about 10% to 25% of the biomass. It has a long-chain, aromatic polymer composed largely of phenyl propane units[12].

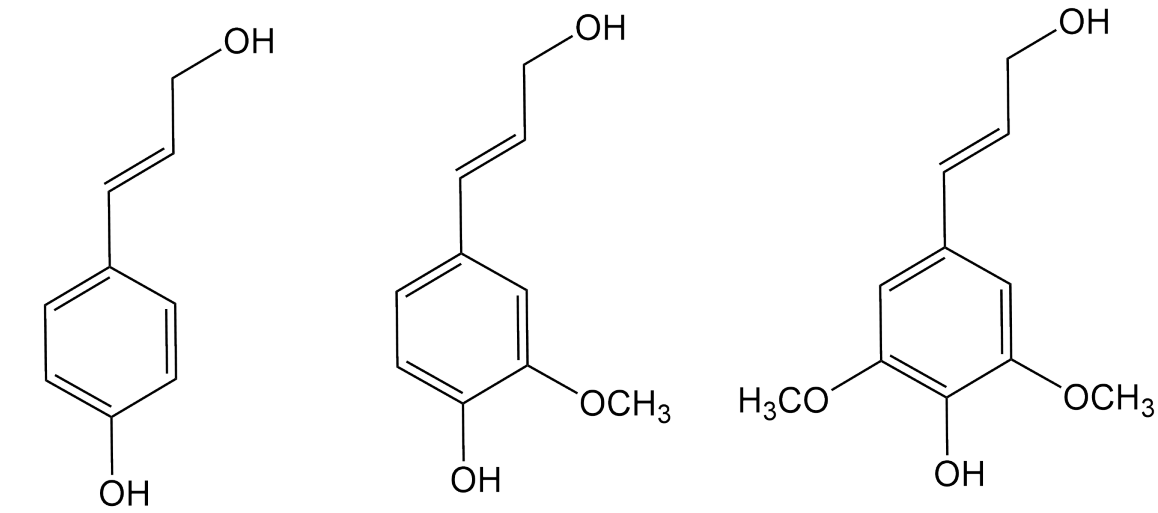

Figure 3.6: Schematic illustration of the lignin main components structures : p-coumaryl alcohol, coniferyl alcohol and synapyl alcohol,drawn with ChewDraw.

Lignins are three-dimensional polymers,which consist of non linearly and randomly linked phenyl propane units.
The main building blocks of lignins are p-hydroxyphenyl (p-coumaryl alcohol) , guaiacyl (coniferyl alcohol) , and syringyl (synapyl alcohol) phenylpropanoid units, which only differ in the degree of methoxylation[10], as showed in the Fig.3.6.

Lignin acts like a glue by filling the gap between and around the cellulose and hemicellulose complexion with the polymers[12].They impart rigidity to the cell wall and resistance to biological decay.Lignins also act as a water resistant adhesive between lignocellulosic cells.[10] It is present in almost all kind of cellulosic plant biomass and acts as a protective sheet against cellulosic and hemicellulosic components of the biomass materials.
Lignin is consists of multifarious and large polymer of phenyl propane, methoxy groups and non-carbohydrate poly phenolic substance, which bind cell walls constituent together[12].

Importance of lignin

The presence of lignins in the tissue structure greatly determines the mechanical and water related properties of wood.Various functions are attributed to lignins:

1. 1. To render wood waterproof. Lignins reduce moisture sorption and cause a higher dimensional stability (restrict swelling and shrinking) compared to non-

lignified tissues (lignin also plays an important role with respect to hysteresis during moisture sorption of wood)

2. 2. To stiffen the cell wall. Lignins lend rigidity and compression strength to the tissue and allow vascular plants to grow upwards.Trees transport the moisture in th wood using a transpiration pull created by transpiration of water through the leaves (transpiration tension).The cell walls can only withstand his high tension(pressure) because lignins impart a high compression strength.

3. 3. To bind wood cells together.Lignins located in the middle lamella act as a kind of water resistant,non hydrolysable adhesive[10].

3.2 Degradation of Wood

Wood modification is an excellent and increasingly used method to expand the application of woody materials. Traditional methods, such as chemical or thermal, have been developed for the targeted improvement of some selected properties, unfortunately typically at the expense of others. These methods generally alter the composition of wood, and thus its mechanical properties; enhance dimensional stability, water resistance, or decrease its susceptibility to microorganisms. Although conventional methods achieve the desired properties, they require a lot of energy and chemicals, therefore research is increasingly moving towards more environmentally friendly processes[13].

Wood changes dimensions with changing moisture content because the cell wall polymers contain hydroxyl and other oxygen-containing groups that attract moisture through hydrogen bonding. The hemicelluloses are mainly responsible for moisture sorption, but the accessible cellulose, non crystalline cellulose, lignin, and surface of crystalline cellulose also play major roles[14].
Alternating swelling and shrinkage due to changing moisture content induces the formation of cracks in wood.Wood with high dimensional stability tends to a lower degree of cracking[10].

In modifying wood for property improvement, one must consider several basic principles when selecting a reagent and a reaction system. Of the thousands of chemicals available, either commercially or by synthetic means, most can be eliminated because they fail to meet the requirements or properties listed below. If hydroxyl reactivity is selected as the preferred modification site, the chemical must contain functional groups, which will react with the hydroxyl groups of the wood components. This happened to be ,the cause for several failed reaction systems in the literature; using a chemical that could not react with a hydroxyl group. The overall toxicity of the chemicals must be carefully considered too. The chemicals must not be toxic or carcinogenic

to humans in the finished product, and should be as nontoxic as possible in the treating stage. The chemical should be as non corrosive as possible to eliminate the need for special stainless steel or glass-lined treating equipment.

In considering the ease with which excess reagents can be removed after treatment, a liquid treating chemical with a low boiling point is advantageous. Likewise, if the boiling point of a liquid reagent is too high, it will be very difficult to remove the chemical after treatment. It is generally true that the lowest member of a homologous series is the most reactive and will have the lowest boiling point. The boiling point range for liquids to be considered is 90–150 °C. In some cases, the lowest member of a homologous series is a gas[14].

A final consideration is, of course, the cost of chemicals and processing. In laboratory scale experimental reactions, the high cost of chemicals is not a major factor. For the commercialization of a process, however, the chemical and processing costs are very important factors. Laboratory scale research is generally done using small batch processing. But rapid, continuous processes should always be studied for scale-up. An economy of scale can make an expensive laboratory process economical[14].

Delignified Wood

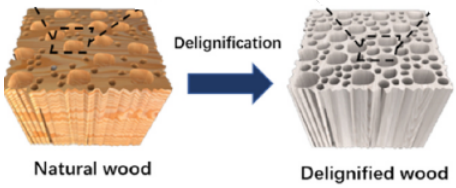

Figure 3.7: Schematic illustration of final look of wood after a successful delignification

The process of delignification makes wood highly hydrophilic with an aligned cellulose structure and free OH groups. These free reactive OH groups,which are arranged naturally as a potential functionalization site and the hierarchically aligned cellulose structure allow DW(Delignified Wood), to be used as a biotemplate for the development of various functional materials. During the last four years, DW was used as a base material in the fabrication of transparent wood, bulk wood materials, membranes, thermal insulators, phase change materials, solar cells, superflexible wood, energy storage materials, textile fibers from wood, and many more applications related to replacing synthetic plastics[8].

This leads to Wood to become very sensitive to moisture or water upon the removal of the hydrophobic structural polymer lignin from the cell wall and the opening of the cellular structure[8].

In wet conditions, DW is extremely flexible and can be easily molded into different shapes. After drying, free OH groups form H-bonds with one another to fix the into a molded shape. After delignification, the fibril aggregates in DW maintain their cell configurations due to the complex nanofibril structure Immediately after delignification, OH groups exhibit weak interactions[8].

The biggest problem of the existing solution-based delignification is that the low lignin delignified wood might be damaged or broken into pieces in the bleaching solutions, because lignin functions as a polymer matrix bonding agent for cellulose fibrils in the cell walls to endow wood with high mechanical strength.
Wood cell walls comprise three ultrastructural domains: the middle lamella, the primary wall, and the secondary wall, among which the middle lamella acts to adhere adjacent cells and is heavily lignified . After delignification, the mechanical strength of the delignified wood is reduced, leading to severe cell wall delamination in the lignin-rich middle lamella and breaking of the delignified wood into pieces by destruction in the bleaching solutions[15].
For example, some wood species, such as pine, break into pieces after $NaClO_2$ solution-based delignification, limiting the number of wood species for transparent wood preparation. In this regard, handling and fabrication of delignified wood with a low lignin content is still challenging[16].
Many methods were used, over the last years, to improve the properties of wood surfaces through modification. Herein, those methods are classified into two categories: chemical methods and carbonization methods; where the latter relied on chemical reactions or interactions to tone the properties of the utmost surface of the treated wood[17].

For this project the methodology followed by a research group was adopted , where a H_2O_2 steam-modified delignification approach is developed[15].
This method has been chosen over other methods, in order to achieve :a green method, that could be reproduced with the least amount of chemical, to guarantee the availability of it, efficiency of the methodology and the safety during the modification. As mentioned in the Chapter 3.2 these principles are very important in order to achieve wood modification for property improvement.

As an oxidant, H_2O_2 can act as an electrophilic or nucleophilic agent, depending on the pH of the reaction medium;in this case H_2O_2 acts as a nucleophile by forming hydroperoxide anions (HOO^-) under alkaline conditions, as shown in Equation 3.1 :

$$H_2O_2 + HO^- \rightleftharpoons H_2O + HOO^- \tag{3.1}$$

The mechanism beside the delignification through H_2O_2 has been depicted in the Fig.3.8 :

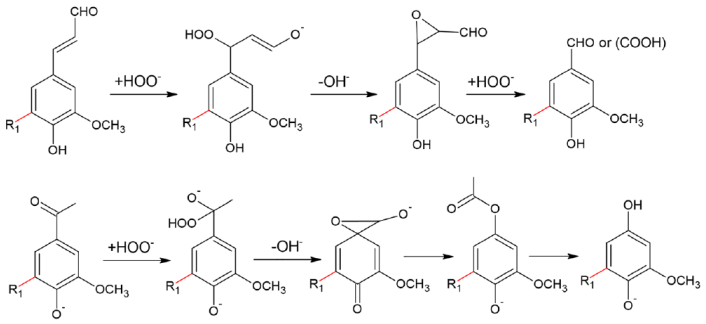

Figure 3.8: Schematic illustration of wood delignification through H_2O_2 drawn with Chem Draw;one of lignin main components, coniferyl alcohol, has been used to present the mechanism.

The reaction proceeds with nucleophilic attack of hydrogen peroxide at Cα position forming an intermediate epoxide. The α-carbonyl structures in phenolic units are quantitatively cleaved to form the corresponding methoxy-hydroquinone derivatives .In the presence of phenolic units, the reaction proceeds via a Dakin-reaction and the intermediate formation of an epoxide,under alkaline conditions, is rapidly hydrolyzed accompanied by cleavage of the Cα–C1 forming the corresponding methoxy hydroquinone derivatives. The mechanism representing this cleavage reactions is shown in Figure 3.8 [18].

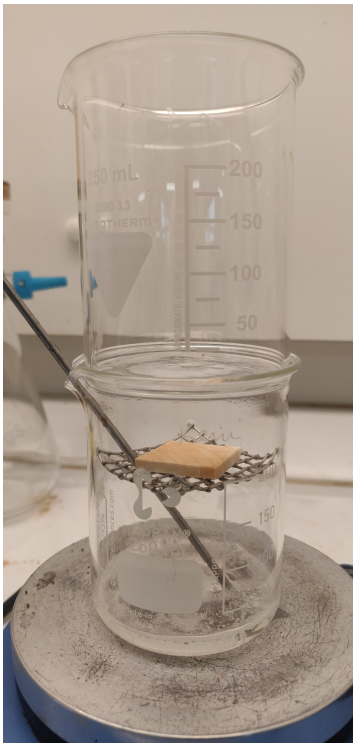

Figure 3.9: Schematic illustration of the setup used to chemical modifications of the samples,reflecting the methodology illustrated in [15]. A thermometer has added in the solution in order to monitor the temperature; another becker has been placed in order avoid the vapor to be dispersed and help the impregnation on of the sample.

Once the modification is completed the DW samples were washed with EtOH first and then water; then placed in a weighing boat and then in the oven to dry , approximately for 8hrs at 50°C. The newly dried wood slices of different sizes (50/25x25mm and the thickness was 4,8 and 12mm) were steamed by placing them on grids with a unit size of 5x5 cm, which were placed above (the distance was approximately 10 cm) a boiling H_2O_2 aqueous solution (33-35 wt%), the whole setup was then covered in order to void vapor dispersion. When the yellow color of the sample disappeared (it took approximately 4–8 h depends on the wood sample thickness), the samples were rinsed with cold water and ethanol.[15]

3.3 Wood-Water interaction

Lignocellulosic materials, like wood, are greatly influenced by the moisture content, and water absorption leads to swelling and changes in all material properties; as mechanical strength, thermal and electric conductivity[19].
Wood will take up or release water, depending on the ambient relative humidity which leads to a complex varying moisture content under natural conditions. Most wood

properties show a strong influence of moisture contents from dry conditions up to the fiber saturation point (FSP, usually defined as the moisture content at which the cell wall is saturated with water, but the lumen are empty). Above the FSP, where added water is held in cell lumen, and therefore not contributing to changes in the cell wall, only properties that are directly influenced by the water content will change, for example the electrical properties[19].
As mentioned ,it is important to understand how moisture enters the wood and how it moves within the wood. Although wood is a porous material (60%–70% void volume), its permeability or flow of water, is extremely variable. This is due to the highly anisotropic arrangement of the component cells and to the variable condition of the microscopic channels between cells. Wood is much more permeable in the longitudinal direction than in the radial or tangential directions; its suggested that a large part of the water in the cell wall may be located in layers around and parallel to the long axis of the cell. It follows that the shrinkage and swelling of the cell-wall will be greatest in the direction perpendicular to the wall;parallel to the grain[20].
Since wood is hygroscopic, it attracts moisture which bonds to the cell wall polymers through hydrogen bonding.

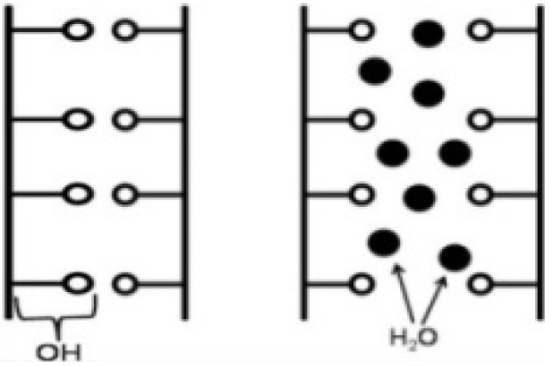

Figure 3.10: Schematic illustration of the Water molecules entering the wood cell wall,depicted from [21]

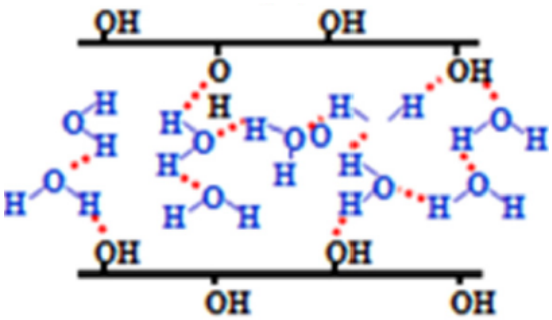

Figure 3.11: Schematic illustration of a fully hydrated cell wall at the fiber saturation point, depicted from [21]

Fig.3.10 shows the mechanism of water molecules adding to the wood cell wall, while Fig.3.11 the fully hydrogen bonded water in the cell.Hydrogen bonds between hydroxyl groups on and between hemicelluloses, cellulose and lignin are constantly changing.

As moisture is added to the cell wall, wood volume increases nearly proportionally to the volume of water added. Swelling of the wood continues until the cell matrix reaches the fiber saturation point (FSP) and water, beyond the FSP, is free water in the void structure and does not contribute to further swelling.
This process is reversible, and wood shrinks as it loses moisture below the FSP. Sorp-

tion of moisture results in swelling/shrinking, cracking, coating failure, and surface degradation.

3.3.1 Water-evaporation induced electricity

In general, wood is mainly composed of cellulose, hemicellulose, and lignin, which are rich in hydroxyl that are on the wood microchannels can be hydrolyzed to appear negatively charged when water infiltrates into the channels.
As a consequence, an electrical potential difference can be built up along the pressure difference direction. Thus, a continuous direct current can be harvested from the water flow driven by natural evaporation. The rationale for using wood to convert evaporation energy into electricity is based on combined theoretical analysis[2].

3.3.2 Mechanisms

The generation of electricity derives from the effect of the streaming potential; but evaporation play a decisive role in the power generation process. When the bottom of the wood surface is placed in water,due to the hydrophilicity and strong capillary force of the inner wood channel, the water climb up along the device and evaporated from the surface and top of the it, and therefore,a stable capillary flow was formed inside the wood channel of device.
When water infiltrate into the wood lumens ,due to the hydrolysis of these hydroxyl groups,these would appear to be negatively charged;by virtue of the attractive force on H+ and the repulsive force on OH^- produced by the negatively charged surface of the wood,an EDL would automatically come into being at the wood/water interface.

When the EDL is overlapped,there would exist massive H+ in the channel of wood which moved with water flow and was enriched at the upper end of the device to establish a polarization distribution as showed in the Fig 3.12.

Driven by a concentration gradient that diffused from the top to bottom,H+ migration opposite to the direction of flow was formed,resulting in a streaming potential[22].
The mechanism of electricity generation from streaming current is shown in the Fig. 3.12

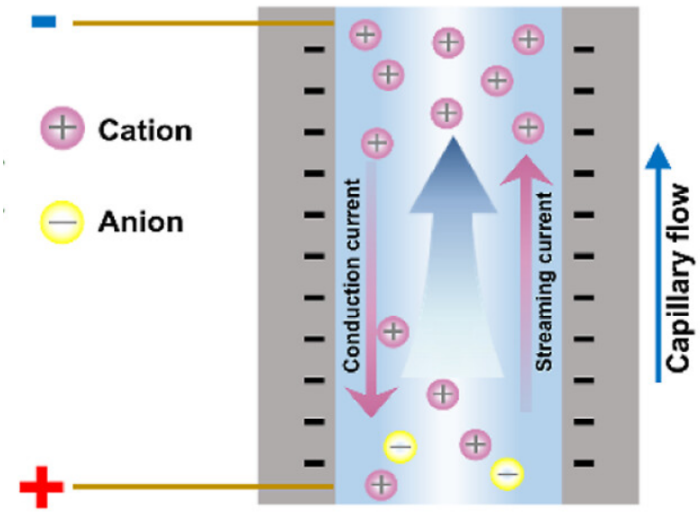

Figure 3.12: Schematic illustration of the mechanism EDL depicted from [22]

Electrical Double layer

As mentioned earlier,streaming potentials are a subset of electrokinetic phenomena, which includes electroosmosis, electrophoresis, and sedimentation potentials. Electrokinetic phenomena are a consequence of a mobile space charge region that exists at the interfacial boundary of two different phases. This region is commonly referred to as the electrical double layer (EDL) [23].

The phenomenon arises because at the wood/water interface a charge distribution often exists where there is an abundance of one species of ions close to the pore wall. The most simplified approximations of the EDL can be represented by a parallel plate capacitor (Helmholtz model) or a charge distribution that decays exponentially away from the surface, Gouy–Chapman model, as showed in Fig 3.13 and Fig.3.14 . A more accurate model takes into account the finite size of ions by combining the Helmholtz and Gouy–Chapman models where a fixed layer exists at the surface (Stern layer) and a diffuse layer extends from the fixed layer into the bulk solution (Gouy–Chapman diffuse layer) as depicted in the Fig3.14.

The figure 3.13 depicts the Stern model which divides the electrical double layer (EDL) into two parts: the Helmholtz layer and the diffuse layer. This gives three planes of interest in the charge distribution of the Stern model:the Stern plane or outer Helmholtz plane (OH),inner Helmholtz plane (IH) and the slipping plane (S).

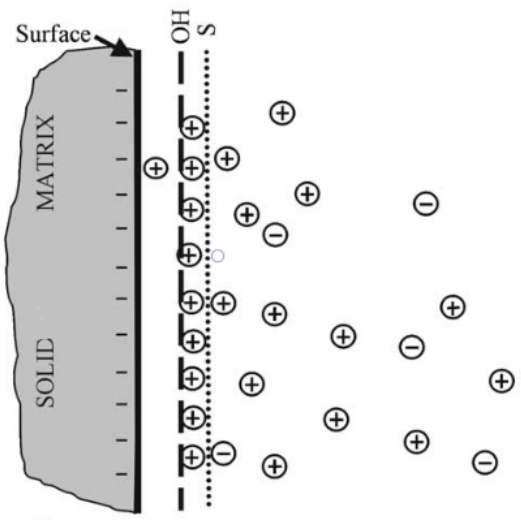

Figure 3.13: Schematic illustration of the the EDL where (OH) is the outer Helmholtz or Stern plane, and(S) is the slipping plane, the diffuse zone is represented by positive ions,depicted from [23]

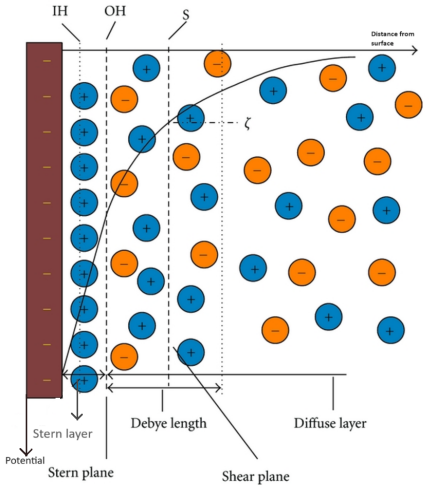

Figure 3.14: Schematic illustration of Gouy–Chapman model illustrated to show the possible potential distributions, and the potentials associated with these three planes of the Stern model. depicted from [23]

The inner Helmholtz plane (IH) is where the ions are adsorbed to the surface; the Stern plane (OH) is the plane where the diffuse layer starts and extends into the bulk fluid, the slipping plane instead,the closest plane to the surface at which fluid motion can take place, is located where the fluid velocity goes to zero when the fluid motion is parallel to the surface. The latter has a potential defined as the Zeta potential(ζ) , which is a characteristic of the solid and liquid that constitute the interface.

Figure 3.14 shows the possible potential distributions, and the potentials associated with these three planes of the Stern model.
The diffuse layer extends from the OH into the bulk of the liquid phase. The distance at which the diffuse layer potential (ψ_0) has been reduced to ψ_0/e is referred to as the Debye length. This is often used as a measure of how far the diffuse layer extends into the bulk fluid[23].
The relative motion between the wood and water, in their interface causes movement of ions parallel to the interface. An electrical convection potential is caused by the movement of the ions, which under equilibrium conditions is balanced by an electrical conduction current where the ions that were moved by the convection current try to return to their original location.

Under many conditions the driving force for the motion of the fluid relative to the solid wall is a differential pressure in the fluid, while the streaming potential signal is the measured voltage. The ratio of the measured voltage across the sample to the

pressure difference across the sample $\Delta V/\Delta P$ is called the streaming potential and is given by the Helmholtz Smoluchowski equation5.5 [23]:

$$\frac{\Delta V}{\Delta P} = \frac{\varepsilon\varepsilon_0\zeta}{\eta\sigma} \tag{3.2}$$

Where ε refers dielectric coefficient of electrolyte ε_0 is the permittivity of the fluid ζ refers to the zeta Potential η refers to the electrolyte viscosity and σ refers to the the fluid conductivity.

4 | Methodology

4.1 Materials

- Wood supplied by the professor
- 5x5cm metallic grid
- Brass Mesh Electrodes
- Rubber bands

4.1.1 Chemicals and solutions

- NaCl was purchased from VWR Chemicals
- H_2O_2 $33 - 35\%$ was purchased from VWR Chemicals
- EtOH $96 - 99\%$ was purchased from VWR Chemicals
- DI Water supplied by the university

4.1.2 Instrumentation

- Multimeter AMPROBE AM-240
- Thermometer
- Magnetic stirrer and heater LLG-RCT

4.1.3 Laboratory Tools

- Becker 250ml
- Weighing basket
- Lab tweezers

4.2 Sample Preparation

The wood samples were cutted with a circular saw machine by the technician in order to obtain the requested sizes for the testings:
The samples thickness chosen were 4, 8 and 12mm as showed in the Fig. 4.1 and the dimensions chosen were,
50/25mm x 25mm(width x height).Typically 10 pieces for each thickness were cutted. New samples they've been eventually re-cutted in case of fracture during the operations or in case the sample used were unusable for further operations after delignification; for example due breaking or fractures.

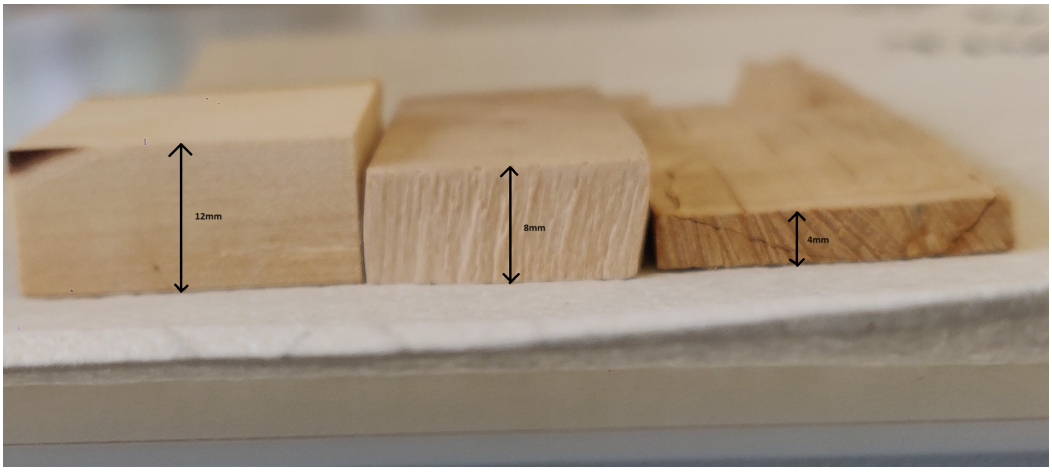

Figure 4.1: Illustration of wood samples different thicknesses used in the experiments.

4.3 Testing

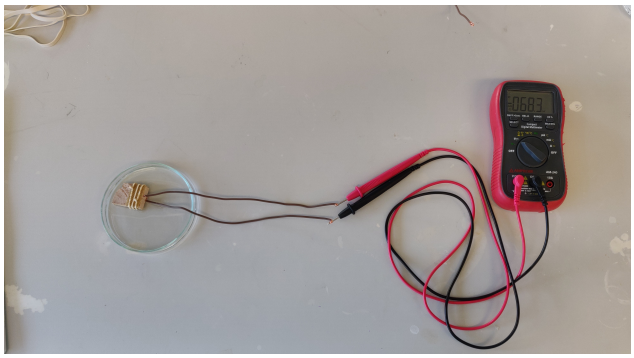

Figure 4.2: Schematic illustration of the setup used for the experiment, with the wood generator placed in a Petri Dish with water, and linked to the multimeter.

Figure 4.3: A closer look ,on the level of wood sample immersed in water during the testings.

For the fabrication of the wood generators , two Brass mesh electrodes were tied on each side of a piece of wood using rubber bands; the generator was then connected through wire cables to the multimeter; the instrument used for the data collection.The device was then placed in a Petri dish ,as depicted in the Fig. 4.2 and water with different temperatures(25 40 and 60°C degrees) was added, to a level just high enough to cover the bottom of the wood, as showed in the Fig.4.3. The volume of water used to fulfill the cover of the wood was determined visually after different trials; 14ml for a thickness of 4mm and 20ml for the other two thicknesses were chosen.

The current and voltage signals from the wood nanogenerators were recorded in real time using a multimeter and the voltage measurement were recorded every minute since the bottom was covered.
They same setup was used to investigate the thickness/temperature and NaCl influence in the harvesting; for the electrolyte a concentration of 200ppm was added in the water before immersing the wood samples. To obtain this concentration 2,8mg of NaCl were measured for a volume of 14ml of water and 4mg for a volume of 20ml.

4.4 Characterization

The microstructure and morphologies of the wood samples, prior and after modifications, are examined by the scanning electron microscope (SEM). The pore size distribution and the porosity of the samples has been observed through the images . The chemical compositions of the samples are characterized by Fourier-transform infrared spectroscopy (FT-IR).

4.4.1 FT-IR

The FT-IR analysis were performed using BRUKER TENSOR II system; in order to examine qualitative and quantitative changes in the wood sample after the delignification; to verify a successful delignification. The instrument operates on the principle that the interference of radiation between two beams creates an interferogram. This interferogram is a signal produced as a function of the path length difference between the two beams, which are reflected from two mirrors positioned within the interferometer block.

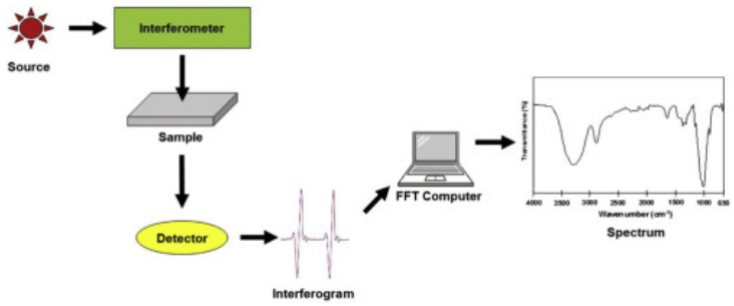

Figure 4.4: Schematic illustration of the FT-IR components.

4.4.2 SEM

The SEM analysis were performed using EVO L15 ZEISS system; in order to examine the microstructure and morphologies of the wood samples, prior and after modifications; to verify a successful delignification. SEM technology operates on the principle of directing a fine beam of high-energy electrons, into the surface of a specimen. By analyzing the various signals generated from the specimen surface, its properties can be determined. The pore size of the specimen has been pointed out in order to emphasizes the eventual successful modification; in addiction the porosity has been calculated from the images with the software IMAGE J.

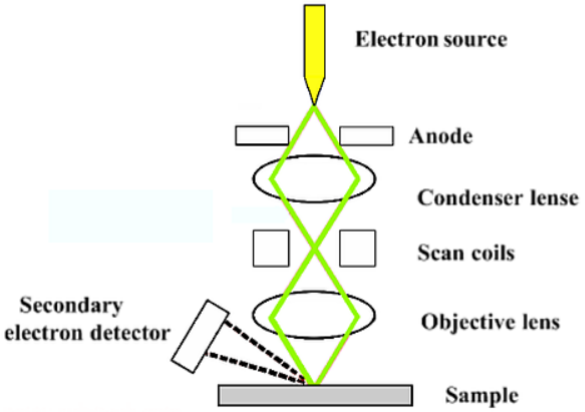

Figure 4.5: Schematic illustration of the SEM components.

5 | Results and discussion

5.1 FTIR spectrum

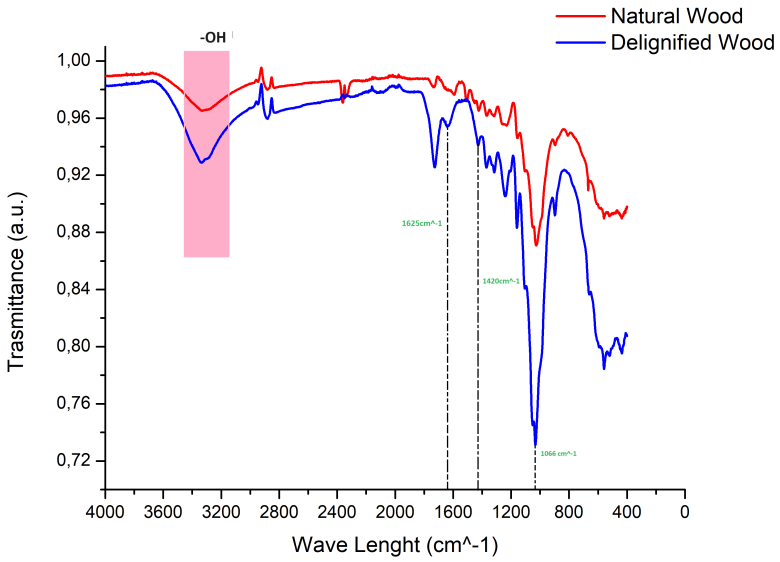

Figure 5.1: FT-IR spectra of untreated and delignified wood.

In the provided Fig. 5.1, the red spectra represents the FT-IR spectrum of normal (untreated) wood, the blue spectra instead, represents the spectrum of delignified wood. To determine a successful delignification, characteristic peaks of lignin, cellulose and hemicellulose are observed:

By examining the graph,there is a noticeable decrease in transmittance (indicative of lower absorption) at the lignin characteristic peaks[24] around 1600 cm^{-1}, 1510 cm^{-1} in the blue spectrum compared to the red spectrum. The peaks around 1050 cm^{-1} and 895 cm^{-1} appear relatively more prominent in the blue spectrum, suggesting an increase in cellulose content relative to lignin.

In case of a unsuccessful delignification, we would observe minimal changes in the intensity of the lignin peaks between the treated and untreated samples, indicating that lignin was not correctly removed. However, based on the provided graph, there is a clear reduction in the lignin peaks, suggesting successful delignification.

In FT-IR spectroscopy, the O-H stretching vibration typically appears as a broad peak due to hydrogen bonding. For wood and other cellulose-containing materials, the O-H stretch is generally observed between 3200 cm^{-1} and 3600 cm^{-1}. The presence of a broad peak in the 3200 cm^{-1} to 3600 cm^{-1} region in both the red and blue spectra confirms the presence of hydroxyl groups. A shape and intensity change, due to the removal of lignin, suggest modifications in the overall hydrogen bonding network.

5.2 SEM images

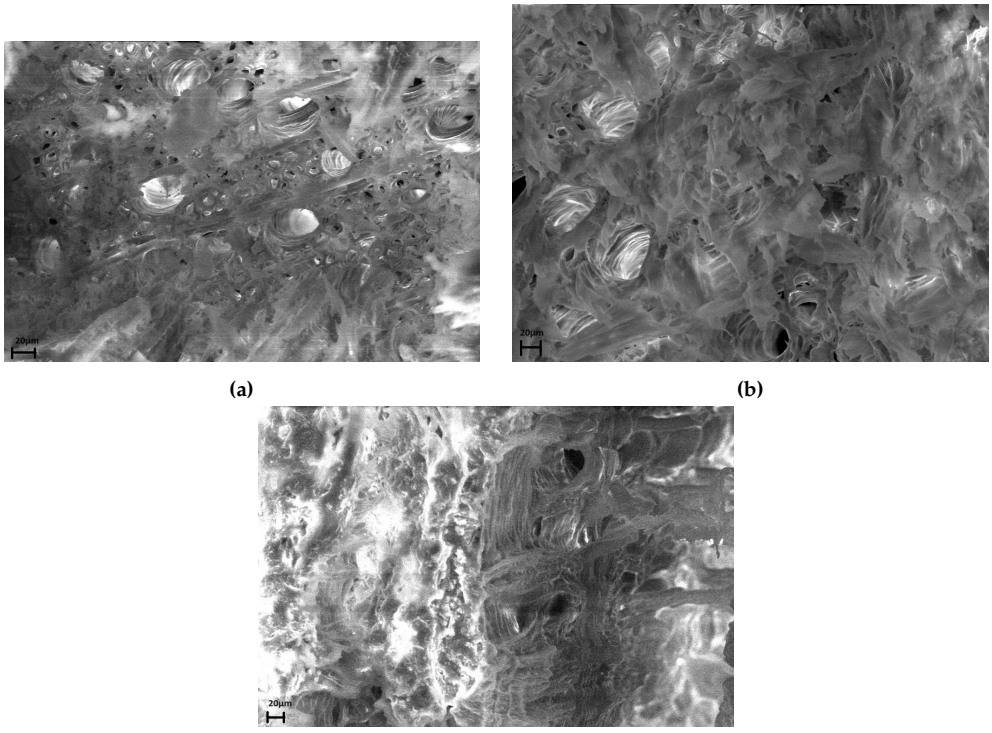

(a) (b)

(c)

Figure 5.2: SEM image of the wood samples untreated(a), delignified(b) and post testing(c), for a 20μ scale.

In the SEM images with a 20μ scale,a visual evaluation of the pore size increase or decrease , pre post or after testing, of the wood samples,has been conducted. By

comparing Fig. 5.2a and Fig. 5.2b , we can observe an increase of the pore size after the delignification; in confirmation of a successful modification. In support to the visual confirmation, the average porosity of the images have been calculated , through a software called ImageJ. By isolating the pores , to be the only subject of interest during the misuration, and then calculating the area size %; a porosity of 31.494% , 37.252% and 31.068% has been calculated respectively for the untreated , delignified and post experiment wood. Therefore ,not only we can state a visual increase in the pores has happened, but this can be supported by an increase in in the porosity. The post testing porosity, shows a decrease from the delignified samples, that might be due the the swelling of the samples during the testing(while be immersed in water) and then the shrinkage of the sample , while placed again in the oven to dry; this may had cause a drop in the porosity of the sample.

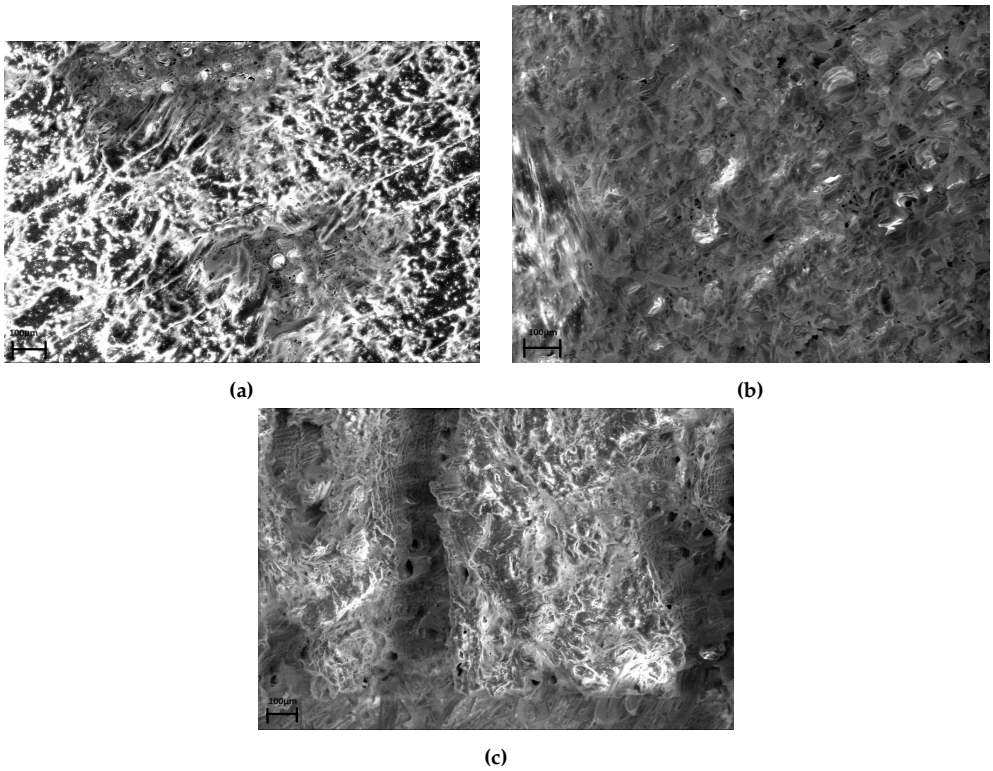

Figure 5.3: SEM image of the wood samples untreated(a), delignified(b) and post testing(c), for a 100μ scale.

In the SEM images with a 100μ scale,a visual evaluation of the pore size increase or decrease, it's quite difficult in comparison to the Fig. 5.2. A higher concentration of pores is show cased both in the Fig. 5.3b and Fig.5.3c in comparison to the Fig. 5.3a ; the latter shows a defined wood grain of samples , that kinda vanish when looking back at the Fig. 5.3b, giving insight of the surface modification performed.

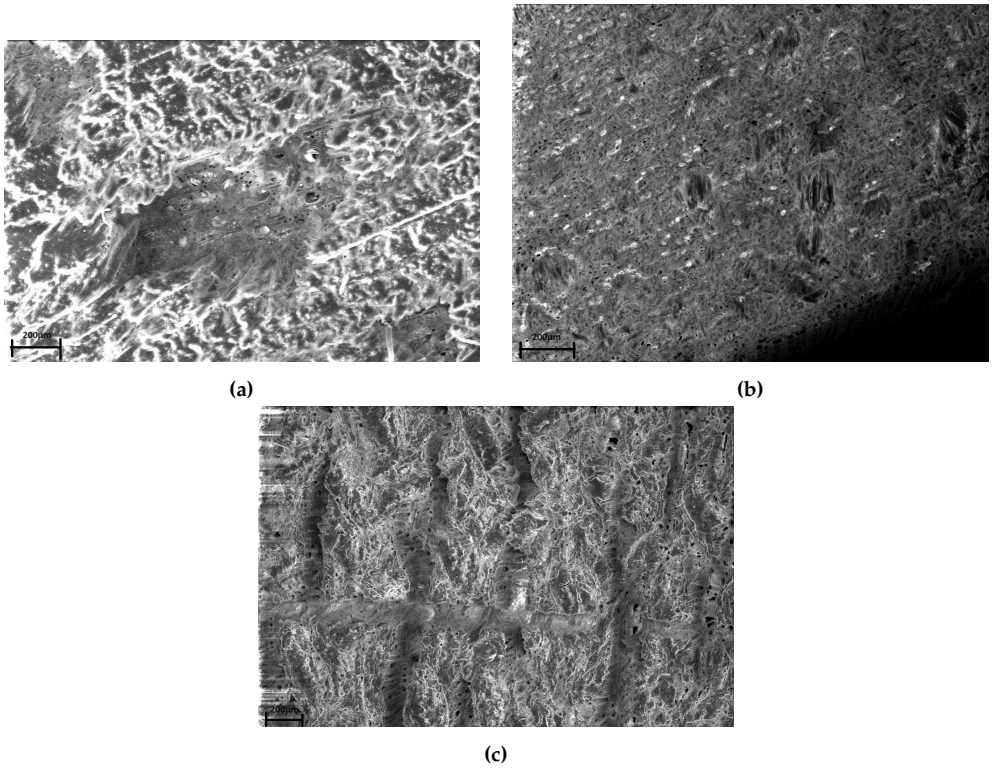

Figure 5.4: SEM image of the wood samples untreated(a), delignified(b) and post testing(c), for a 200μ scale.

Differently from the 20μ we cannot visually observe pore size and and have an evaluation of a reduction or an increase of it; but we still can clearly observe the presence of a higher concentration of pores, either in the delignified wood and sample tested post testing, in comparison, to the untreated wood ; to utmostly confirm the successful modification.

5.3 Temperature and thickness influence in power generation

The data collected over time ,though the multimeter, has been plotted to obtain the graphs showed below.

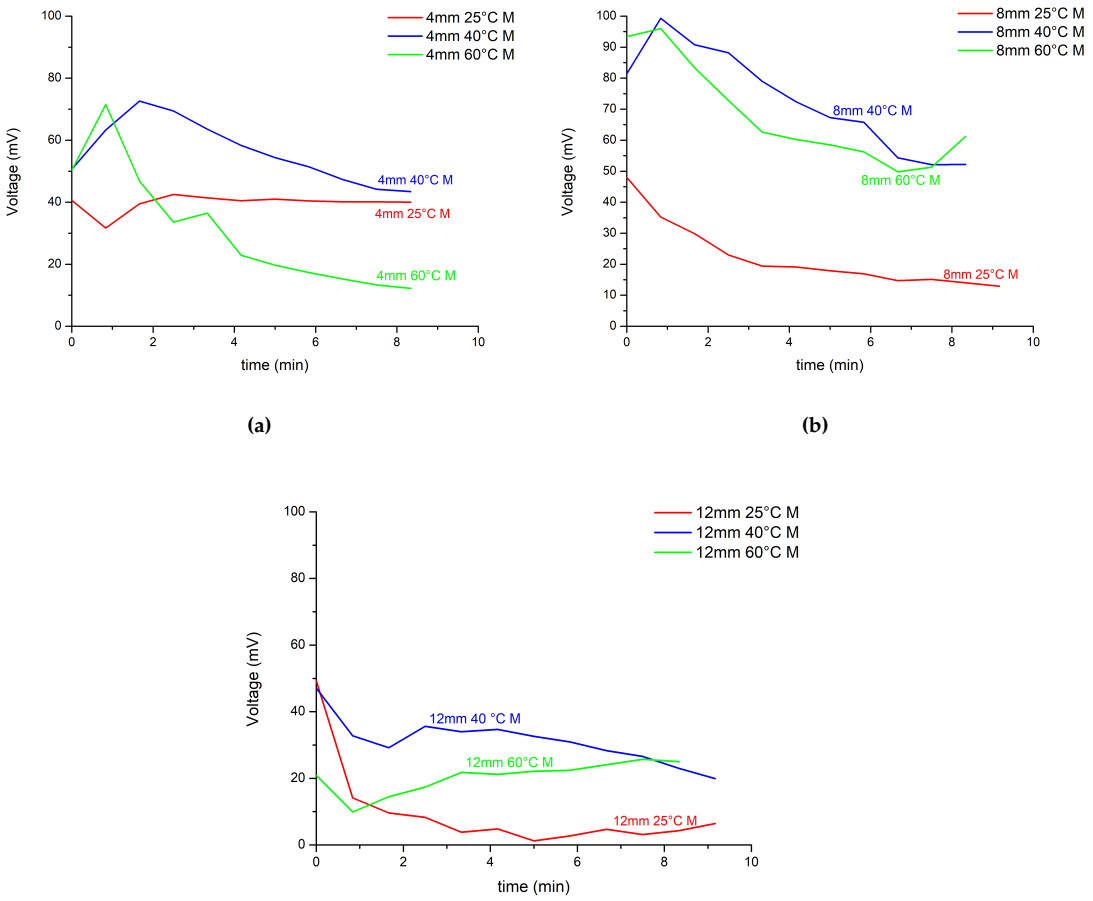

Figure 5.5: Voltage output over time for a 4mm(a) ,8mm(b), 12mm(c) DW samples ,in order to evaluate the influence of different temperatures of water used for the harvest:

How different temperatures and thickness affects the DW sample voltage output(V_o) has been observed:

To fully understand the voltage output , theoretical consideration has to been keep in mind;
As the wood sample is tide in two electrodes , and immersed in water with different temperatures, between the two electrodes a change of heat occur. Heat conduction is the transfer of thermal energy through a material due to a temperature gradient, where heat flows from a region of higher temperature to a region of lower temperature [25], in this case from the electrode immersed in water and the one in the upper part of the wood.

Across the wood a temperature gradient forms up ,and can be defined as :

$$\Delta T = \frac{dT}{dx} \tag{5.1}$$

Given the boundary conditions in the setup:

At x=0: $T = T_{air}$ (temperature of the air-exposed side).
At x=L: $T = T_{water}$ (temperature of the water-immersed side).

We can define the gradient as :

$$\Delta T = \frac{dT}{dx} = \frac{T_{water} - T_{air}}{L} \tag{5.2}$$

Where
L is the wood thickness

Trough the temperature gradient formed, the voltage can be determined referring to the Seebeck Effect.
The Seebeck effect is a thermoelectric phenomenon in which a temperature difference across a material generates an electric voltage; the voltage is proportional to the temperature difference and the Seebeck coefficient of the material as depicted in the following equation:

$$V = \Delta T \cdot S_c \tag{5.3}$$

Where:

S_c is the Seebeck coefficient.
ΔT is the temperature difference across the thickness.

We can then write the equation as :

$$V = \frac{T_{water} - T_{air}}{L} \cdot S_c \tag{5.4}$$

By investigating the differents graphs showed in Fig. 5.5:
We can observe how for the three graphs the thickness of the wood sample has been kept constant for a better evaluation of temperature influence.
By keeping a parameter like the thickness constant, and referring to the Eq.5.3, and keeping the S_c constant as the material doesn't change , we can say that the V_o depends mainly from the temperature; and we would therefore expect an increase of the voltage proportional to the increase of the temperature. By looking at the Fig.5.5b and 5.5c

we can see this theory is followed , where the 60°C graphs gives a lower V_o compared to the 40°C, but progressively over time shows the highest one; but probably the time of observation is not sufficient to completely determine the following behaviour. this trend doesn't follow Fig. 5.5a where the highest temperature shows the lowest V_o.
This anomaly could be commented with different potential explanations include:

1. A non-Uniform temperature Distribution: Variations in the thermal conductivity or physical properties of the wood could lead to an uneven temperature gradient. The interface between the wood and the brass mesh electrodes might not be consistent, affecting heat transfer.

2. Contact Resistance: Different contact resistances at the water-immersed and air-exposed electrodes can alter the effective temperature gradient. Poor thermal contact at one of the interfaces could lead to a lower ΔT than expected.

3. Measurement Inconsistencies: Variations in the experimental setup, such as differences in immersion depth or air flow around the air exposed electrode, could affect the temperature distribution. Calibration or alignment issues with the multimeter or wires could lead to inaccurate voltage readings.

4. Structural changes After the delignification the wood samples may incur in variations in its structure or composition that affect its thermoelectric properties. Inhomogeneities can lead to irregularities in the voltage generated, especially if certain areas have different Seebeck coefficients.

A further observation could be made by analyzing the behavior of the different graphs: all of them progressively reach a peak within the the first 2min of time of observation; to an eventual progressive and steady decrease in the V_o. These actions can be explained by referring to the Gouy Chapman model in Chapter3.3.2, where from the observation of the Fig.3.14 we can deduct potential decay of the potential as we increase the distance from the surface; phenomenon that occurs when the ions starts from the bottom of the wood (in contact with water) to reach the top of it.

5.4 Nacl addiction influence

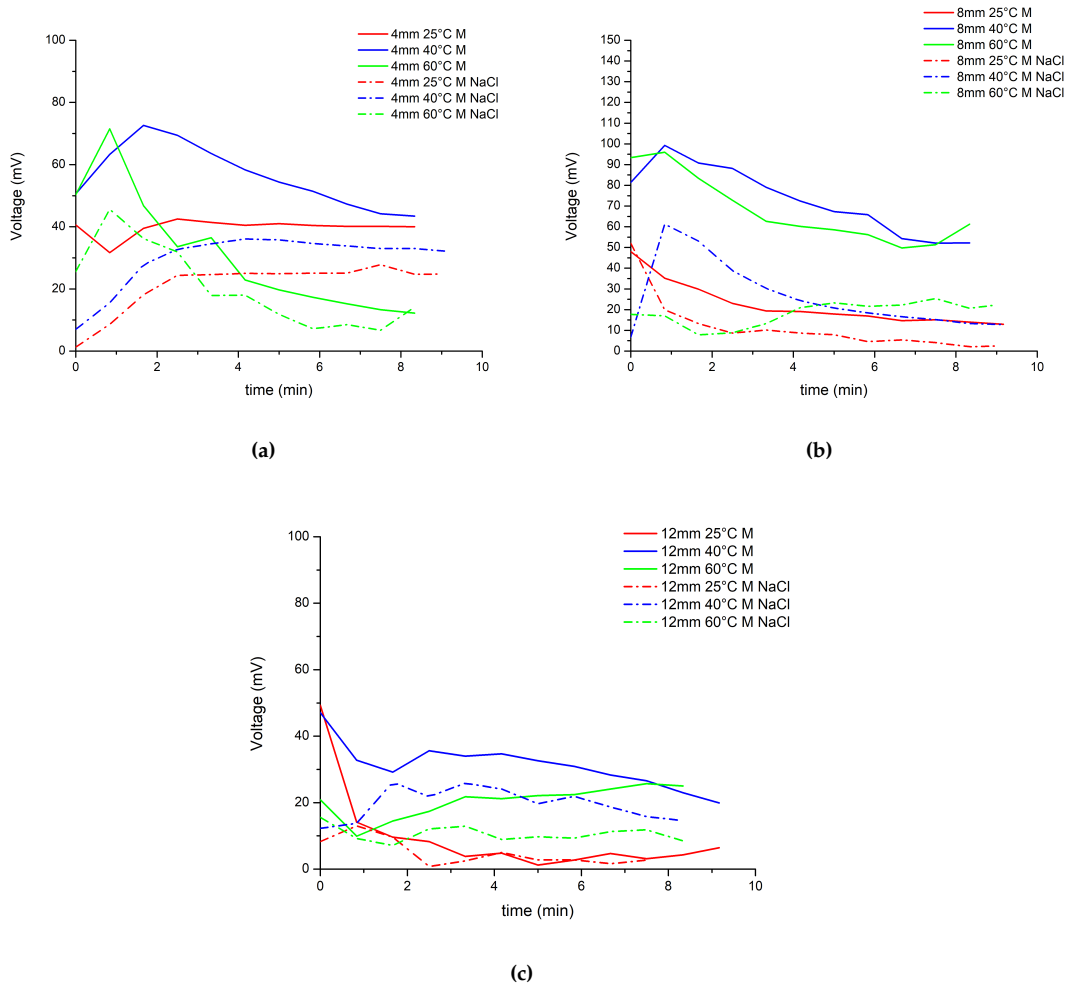

Figure 5.6: Voltage output over time for a DW sample in order to evaluate the Nacl addiction in water,influence.Different temperatures has been observed 25(a), 40(b) and 60(c):

The possible influence, of the addiction of an electrolyte like Nacl, in the water used to harvest with wood, has been investigated through the Fig.5.6 ,over reported. For each one of the graphs its clearly depictable the lower voltage output produced during the testing with the addiction NaCl ; this phenomenon can be explained through a series of theoretical and mathematical consideration; below discussed:
As mentioned in the Chapter 3.3.2, the streaming potential can be determined through the equation :

$$\frac{\Delta V}{\Delta P} = \frac{\varepsilon \varepsilon_0 \zeta}{\eta \sigma} \tag{5.5}$$

In the same chapter , the Debye Length has been defined too; as the distance at which the diffuse layer potential (ψ) has been reduced to ψ/e. Mathematically speaking it can be expressed by using the Debye Huckel parameter,referred as κ,obtained by the linearization of the Poisson-Boltzmann equation,that describes the electrostatic potential distribution in the electrical double layer:

$$\kappa = \sqrt{\frac{2N_a e^2 I}{\varepsilon_0 \varepsilon \kappa_B T}} \tag{5.6}$$

Where:
N_a refers to the Avogadro Number
e refers to the elementary charge
I refers to the Ionic Strength
ε_0 refers to the permittivity of the fluid
ε refers to the dielectric coefficient
κ_B refers to the Boltzmann constant
T refers to the Temperature

Through this parameter the Debye Length λ_D can be defined as:

$$\lambda_D = \frac{1}{\kappa} \tag{5.7}$$

The Ionic Strength in particular, defined as a measure of the concentration of electrically charged species in solution , can be expressed with following equation:

$$I = \frac{1}{2} \sum z_i^2 c_i \tag{5.8}$$

Where z_i refers to the valence of the ions and c_i refers to the ions concentration.
So when observing an 1:1 electrolyte like NaCl , z_- and z_+ are both $\pm$ 1, and if c_+ and c_- are the concentrations of the cation and anion respectively; the Ionic Strength can be calculated and expressed as :

$$I = \frac{1}{2} \sum z_i^2 c_i = \frac{1}{2} \left\lfloor c_- \cdot 1^2 + c_+ \cdot 1^2 \right\rfloor = \frac{1}{2} (c + c) = c \tag{5.9}$$

Known most the values of the5.4 , for the case of a 1:1 electrolyte, κ can be reduced to:

$$\kappa = \frac{\sqrt{I}}{0,303} \tag{5.10}$$

And this emphasize even more the influence of the concentration of an electrolyte over κ.As the concentration increase, even κ increase and due the inverse proportional relationship with λ_D, the debye length decrease. As the concentration of salt increase

another effects is depictable, as the value of absolute zeta potential decreased due to charge screening in electrical double layer[26].
As defined in the Chapter3.3 the zeta potential is the is the potential of the slipping plane, and knowing the zeta potential is important for the characterization of electrochemical surface properties[26]. The zeta potential can be defined as:

$$\zeta = \zeta_0 \cdot e^{-\kappa x} \tag{5.11}$$

Where:
ζ_0 is the zeta potential at low ionic strength.
κ is the inverse Debye length
x is the distance from the surface.

At the shear plane, the distance x is characteristic of the double layer thickness, typically approximated as $x \simeq \lambda_D \simeq \frac{1}{\kappa}$. Hence:

$$\zeta = \zeta_0 \cdot e^{-1} \tag{5.12}$$

However, a more precise model considering non-linear screening is given by:

$$\zeta = \zeta_0 \cdot \tanh(\kappa d) \tag{5.13}$$

Since κ increases with concentration, $\tanh(\kappa d)$ approaches 1, but for practical concentrations, ζ still decreases.
Given that the streaming potential (ΔV) is directly proportional to the zeta potential (ζ) as shown in the equation 5.5; as the concentration increases, the decrease in zeta potential (ζ) leads to a decrease in the streaming potential. The more ions are present in the solution, the more they screen the surface charge, reducing the effective zeta potential and thus reducing the streaming potential.

6 | Conclusion

The project aim , was to develop a method to convert low grade heat , such the ambient heat, in usable forms of power and water production;this goal has been achieved.
Wood generators to draw electricity from natural evaporation, has been successfully fabricated. It is based on rational design using streaming potential/current and capillary pressure to harvest electricity. Properties and reason to investigate wood has been described. The theoretical and mathematical side of the electricity generation has been scrutinized trough equations as the Helmholtz-Smoluchowski, Poisson Boltzmann; and models as the Stern model and the Electrical Double Layer. The influence of the samples thickness and the water temperature has been investigated and commented, trough the report; resulting in 8mm 40°C being the best temperature/thickness combination to perform the highest voltage output. The correct modification of the wood sample has been established through characterization analyses as the SEM ,by observing visually the microstructure and morphologies of the wood samples, and FT-IR to observe the chemical compositions through the modifications processes.

7 | Perspectives

Spontaneous methods of electricity harvesting that only utilize ambient energy have been widely explored in recent years; hence ,this topic opens the doors to various possible insights: as mentioned,the wood chemical modification is an excellent and increasingly used method to expand the application of woody materials; in literature not many modification to render wood more hydrophilic have been studied, that could even be possibly, not toxic and easily reproducible,is in that occurrence that exploring modification used for other materials ,with kinda similar characteristics, could help in this purpose.
Regards some possible additional modifications to increase the capabilities of these wood generators, could have been a nanoparticles insertion. Minerals, such as ZnO and Fe_3O_4 are beneficial for efficient water evaporation, further contributing to enhanced power generation.
Formation of a hierarchical nanostructure of iron oxides is attractive yet challenging. There's hypothesis that combining iron oxides with a hierarchical structure of wood could provide the possibility to solve the issues and achieve efficient hydrovoltaic power generation. Unfortunately due the absence of the instruments needed to perform a vacuum infiltration,that could ensure a homogeneous distribution throughout the whole wood, this option couldn't be pursued , but its worth to consider , in case of further investigations in this topic.
Wood sample wise , consideration regards the use of different thickness and different water temperatures could be made. Thin wood samples of 2mm has been tried to test , but probably the modification through H_2O_2 was too harsh for this thickness, leading to breaking of the sample once with the modification , or even during the washing with water/ethanol. An intermediate thickness between 2 and 4 could be observed. The effects of the temperature in the experiments has been remarked in the Experimental Section (Chapter n°5), tests with water temperatures lower and higher than the one used in the report could be effectuated to corroborate or find deviations concerning the observations made in that chapter.
The implementation of membrane could probably ensure additional experiments. After a verification of the correct functioning of our wood generators, replication of the characteristics of the sample(pore size >1μm and a thickness in the order of mil-

limeters) and then choosing the membrane type of interest (es. ceramic, polymer), the usage of a 3D printer could be taken in consideration,to create membrane as a mimic of wood. The 3D printer disponible in the laboratory, couldn't unfortunately reproduce those parameters as the resulting membrane would possess a flat sheet instead of the tubular one, showed by the wood samples.This option could push the experimentations in the world of PWID s(Portable wearable implantable electronic devices) taking advantage of the higher flexibility of the membranes in comparison to the wood. As a further exploration of this topic , the water evaporated through the wood could be tried to be collected in through a system linked to the setup used to produce voltage,in order to ,render the wood sample, a generator of power and fresh water; as beneficial to the current different request for sustainable wastewater treatments.

Bibliography

[1] K. Jiao, H. Yan, F. Qian, *et al.*, "Energy harvesting based on water evaporation-induced electrokinetic streaming potential/current in porous carbonized carrots," *Journal of Power Sources*, vol. 569, p. 233 007, Jun. 2023, ISSN: 0378-7753. DOI: 10.1016/j.jpowsour.2023.233007. [Online]. Available: http://dx.doi.org/10.1016/j.jpowsour.2023.233007.

[2] X. Zhou, W. Zhang, C. Zhang, *et al.*, "Harvesting electricity from water evaporation through microchannels of natural wood," *ACS Applied Materials amp; Interfaces*, vol. 12, no. 9, 11232–11239, Feb. 2020, ISSN: 1944-8252. DOI: 10.1021/acsami.9b23380. [Online]. Available: http://dx.doi.org/10.1021/acsami.9b23380.

[3] Z. Zhang, X. Li, J. Yin, *et al.*, "Emerging hydrovoltaic technology," *Nature Nanotechnology*, vol. 13, no. 12, 1109–1119, Dec. 2018, ISSN: 1748-3395. DOI: 10.1038/s41565-018-0228-6. [Online]. Available: http://dx.doi.org/10.1038/s41565-018-0228-6.

[4] X. Zhao, Z. Xiong, Z. Qiao, *et al.*, "Robust and flexible wearable generator driven by water evaporation for sustainable and portable self-power supply," *Chemical Engineering Journal*, vol. 434, p. 134 671, Apr. 2022, ISSN: 1385-8947. DOI: 10.1016/j.cej.2022.134671. [Online]. Available: http://dx.doi.org/10.1016/j.cej.2022.134671.

[5] Z. Zhang, Y. Zheng, N. Jiang, *et al.*, "Electricity generation from water evaporation through highly conductive carbonized wood with abundant hydroxyls," *Sustainable Energy amp; Fuels*, vol. 6, no. 9, 2249–2255, 2022, ISSN: 2398-4902. DOI: 10.1039/d2se00309k. [Online]. Available: http://dx.doi.org/10.1039/d2se00309k.

[6] L. Hällström, T. Koskinen, C. Tossi, T. Juntunen, and I. Tittonen, "Multiphysics simulation explaining the behaviour of evaporation-driven nanoporous generators," *Energy Conversion and Management*, vol. 256, p. 115 382, Mar. 2022, ISSN: 0196-8904. DOI: 10.1016/j.enconman.2022.115382. [Online]. Available: http://dx.doi.org/10.1016/j.enconman.2022.115382.

[7] Q. Fu, Y. Chen, and M. Sorieul, "Wood-based flexible electronics," *ACS Nano*, vol. 14, no. 3, 3528–3538, Feb. 2020, ISSN: 1936-086X. DOI: 10.1021/acsnano.9b09817. [Online]. Available: http://dx.doi.org/10.1021/acsnano.9b09817.

[8] A. Kumar, T. Jyske, and M. Petrič, "Delignified wood from understanding the hierarchically aligned cellulosic structures to creating novel functional materials: A review," *Advanced Sustainable Systems*, vol. 5, no. 5, Mar. 2021, ISSN: 2366-7486. DOI: 10.1002/adsu.202000251. [Online]. Available: http://dx.doi.org/10.1002/adsu.202000251.

[9] D. E. Kretschmann, "Mechanical properties of wood," *Environments*, vol. 5, p. 34, 2010.

[10] D. S. Peter Niemz Alfred Teischinger, *Springer Handbook of Wood Science and Technology*. Springer Nature Switzerland, 2023, ch. Chemical Modification of Wood.

[11] *Handbook of Wood Chemistry and Wood Composites*. CRC Press, Sep. 2012, ISBN: 9780429109096. DOI: 10.1201/b12487. [Online]. Available: http://dx.doi.org/10.1201/b12487.

[12] T. Shahzadi, S. Mehmood, M. Irshad, *et al.*, "Advances in lignocellulosic biotechnology: A brief review on lignocellulosic biomass and cellulases," *Advances in Bioscience and Biotechnology*, vol. 05, no. 03, 246–251, 2014, ISSN: 2156-8502. DOI: 10.4236/abb.2014.53031. [Online]. Available: http://dx.doi.org/10.4236/abb.2014.53031.

[13] S. Klébert, M. Mohai, and E. Csiszár, "Can plasma surface treatment replace traditional wood modification methods?" *Coatings*, vol. 12, no. 4, p. 487, Apr. 2022, ISSN: 2079-6412. DOI: 10.3390/coatings12040487. [Online]. Available: http://dx.doi.org/10.3390/coatings12040487.

[14] R. M. Rowell, *WOOD CHEMISTRY AND WOOD COMPOSITES*. USDA Forest Service Forest Products Laboratory and Department of Biological Systems Engineering, University of Wisconsin Madison, WI, 2005, ch. Chemical Modification of Wood.

[15] H. Li, X. Guo, Y. He, and R. Zheng, "A green steam-modified delignification method to prepare low-lignin delignified wood for thick, large highly transparent wood composites," *Journal of Materials Research*, vol. 34, no. 6, 932–940, Feb. 2019, ISSN: 2044-5326. DOI: 10.1557/jmr.2018.466. [Online]. Available: http://dx.doi.org/10.1557/jmr.2018.466.

[16] Y. Li, Q. Fu, R. Rojas, M. Yan, M. Lawoko, and L. Berglund, "Lignin-retaining transparent wood," *ChemSusChem*, vol. 10, no. 17, 3445–3451, Aug. 2017, ISSN: 1864-564X. DOI: 10.1002/cssc.201701089. [Online]. Available: http://dx.doi.org/10.1002/cssc.201701089.

[17] P. Blanchet and S. Pepin, "Trends in chemical wood surface improvements and modifications: A review of the last five years," *Coatings*, vol. 11, no. 12, p. 1514, Dec. 2021, ISSN: 2079-6412. DOI: 10.3390/coatings11121514. [Online]. Available: http://dx.doi.org/10.3390/coatings11121514.

[18] A. More, T. Elder, and Z. Jiang, "A review of lignin hydrogen peroxide oxidation chemistry with emphasis on aromatic aldehydes and acids," *Holzforschung*, vol. 75, no. 9, 806–823, Mar. 2021, ISSN: 0018-3830. DOI: 10.1515/hf-2020-0165. [Online]. Available: http://dx.doi.org/10.1515/hf-2020-0165.

[19] Nopens, Wadsö, Ortmann, Fröba, and Krause, "Measuring the heat of interaction between lignocellulosic materials and water," *Forests*, vol. 10, no. 8, p. 674, Aug. 2019, ISSN: 1999-4907. DOI: 10.3390/f10080674. [Online]. Available: http://dx.doi.org/10.3390/f10080674.

[20] J. B. Boutelje, "The relationship of structure to transverse anisotropy in wood with reference to shrinkage and elasticity," *Holzforschung*, vol. 16, no. 2, 33–46, Jan. 1962, ISSN: 1437-434X. DOI: 10.1515/hfsg.1962.16.2.33. [Online]. Available: http://dx.doi.org/10.1515/hfsg.1962.16.2.33.

[21] R. Rowell and F. Bongers, "Coating acetylated wood," *Coatings*, vol. 5, no. 4, 792–801, Nov. 2015, ISSN: 2079-6412. DOI: 10.3390/coatings5040792. [Online]. Available: http://dx.doi.org/10.3390/coatings5040792.

[22] W. Hong, Y. Zheng, C. Hao, *et al.*, "Surface carbonized natural wood via hydrogen–oxygen flame for electricity generation from water evaporation," *ACS Applied Engineering Materials*, vol. 1, no. 7, 1719–1729, Jun. 2023, ISSN: 2771-9545. DOI: 10.1021/acsaenm.3c00112. [Online]. Available: http://dx.doi.org/10.1021/acsaenm.3c00112.

[23] P. M. Reppert and F. D. Morgan, "Temperature-dependent streaming potentials: 1. theory," *Journal of Geophysical Research: Solid Earth*, vol. 108, no. B11, Nov. 2003, ISSN: 0148-0227. DOI: 10.1029/2002jb001754. [Online]. Available: http://dx.doi.org/10.1029/2002JB001754.

[24] Z. Lou, C. Yuan, Y. Zhang, *et al.*, "Synthesis of porous carbon matrix with inlaid fe3c/fe3o4 micro-particles as an effective electromagnetic wave absorber from natural wood shavings," *Journal of Alloys and Compounds*, vol. 775, 800–809, Feb. 2019, ISSN: 0925-8388. DOI: 10.1016/j.jallcom.2018.10.213. [Online]. Available: http://dx.doi.org/10.1016/j.jallcom.2018.10.213.

[25] Y. HIKI, H. TAKAHASHI, and Y. KOGURE, "An experimental method for studying thermal transport in condensed matter.," *Proceedings of the Japan Academy, Series B*, vol. 69, no. 3, 51–54, 1993, ISSN: 1349-2896. DOI: 10.2183/pjab.69.51. [Online]. Available: http://dx.doi.org/10.2183/pjab.69.51.

[26] S. Salgın, U. Salgın, and S. Bahadır, "Zeta potentials and isoelectric points of biomolecules: The effects of ion types and ionic strengths," *International Journal of Electrochemical Science*, vol. 7, no. 12, 12404–12414, Dec. 2012, ISSN: 1452-3981. DOI: 10.1016/s1452-3981(23)16554-0. [Online]. Available: http://dx.doi.org/10.1016/S1452-3981(23)16554-0.

A Appendix